Bioorganic & Medicinal Chemistry 20 (2012) 2527–2534

Contents lists available at SciVerse ScienceDirect

Bioorganic & Medicinal Chemistry

journal homepage: www.elsevier.com/locate/bmc

Design, synthesis and evaluation of isaindigotone derivatives as dual inhibitors for acetylcholinesterase and amyloid beta aggregation

Jin-Wu Yan, Yan-Ping Li, Wen-Jie Ye, Shuo-Bin Chen, Jin-Qiang Hou, Jia-Heng Tan *, Tian-Miao Ou, Ding Li, Lian-Quan Gu, Zhi-Shu Huang *

School of Pharmaceutical Sciences, Sun Yat-sen University, Guangzhou 510006, PR China

ARTICLE INFO

Article history:
Received 2 January 2012
Revised 25 February 2012
Accepted 27 February 2012
Available online 7 March 2012

Keywords:
Isaindigotone derivatives
AChE inhibition
Aβ aggregation inhibition
Anti-Alzheimer agents

ABSTRACT

A series of isaindigotone derivatives and analogues were designed, synthesized and evaluated as dual inhibitors of cholinesterases (ChEs) and self-induced β-amyloid (Aβ) aggregation. The synthetic compounds had IC_{50} values at micro or nano molar range for cholinesterase inhibition, and some compounds exhibited strong inhibitory activity for AChE and high selectivity for AChE over BuChE, which were much better than the isaindigotone derivatives previously reported by our group. Most of these compounds showed higher self-induced Aβ aggregation inhibitory activity than a reference compound curcumin. The structure–activity relationship studies revealed that the derivatives with higher inhibition activity on AChE also showed higher selectivity for AChE over BuChE. Compound **6c** exhibiting excellent inhibition for both AChE and self-induced Aβ aggregation was further studied using CD, EM, molecular docking and kinetics.

1. Introduction

Alzheimer's disease (AD) is a progressive neurodegenerative brain disorder which is affecting millions of elder people, and the number of patients is expected to reach 70 million by 2050.[1–3] Although many factors have been implicated in AD, its etiology is not completely clear. There are diverse pathologic factors responsible for the AD, such as low levels of acetylcholine, β-amyloid (Aβ) deposits and Tau-protein aggregation.[4,5] Current treatment of AD with AChE (Acetylcholinesterase) inhibitors (tacrine, donepezil, rivastigmine and galantamine) and an NMDA (*N*-methyl D-aspartate) antagonist memantine could only improve symptoms but not address AD's etiology, therefore, much effort has been made to develop more effective drug for the treatment of AD.[6,7]

Among the diverse pathologic factors, ACh and Aβ both play significant roles in the disease. The observation of a deficiency in cholinergic neurotransmission in AD has led to the statement of cholinergic hypothesis. Two types of ChE enzymes have been found in the central nervous system, including acetylcholinesterase (AChE) and butyrylcholinesterase (BuChE), and current treatment of AD mainly focuses on the inhibition of AChE activity in order to rectify the deficiency of cerebral acetylcholine.[8] AChE plays a pivotal role in central and peripheral nervous systems, and its main function is to terminate the impulse transmission at cholinergic synapses. Recent studies have identified that AChE could also play a key role in accelerating senile amyloid β-peptide (Aβ) plaques deposition.[9] AChE has a catalytic site (CAS) at the bottom of deep narrow gorge and a peripheral anionic site (PAS) at the entrance.[10] The simultaneous binding to both sites has been suggested to be important in designing powerful and selective AChE inhibitors.

On the other hand, the amyloid cascade hypothesis implies that the progressive deposition of Aβ is fundamental to the development of neurodegenerative pathology. The cell toxicity associated with Aβ fibril aggregation provides an explanation for the neuronal cell loss found in AD patients. Inhibition of Aβ fibril aggregation has been proved to be a promising approach for the treatment of AD.[11–13] Meanwhile, due to the multi-pathogenesis of AD, an attractive strategy is to develop novel anti-Alzheimer agents with multiple functions. In recent years, many series of promising compounds have been designed and developed to inhibit both AChE and Aβ aggregation.[14–16]

Isaindigotone (**a**, Fig. 1) is a naturally occurring alkaloid which is commonly used in traditional Chinese medicine.[17] The structure of isaindigotone is consisted of a deoxyvasicinone moiety conjugated with a substituted benzylidene moiety. The structure of deoxyvasicinone (**b**, Fig. 1) is similar to that of tacrine (**c**, Fig. 1). In recent years, some deoxyvasicinone derivatives have been found to be ChE inhibitors with a wide range of ChE inhibition activity.[18,19] Our research group has designed and synthesized a series of isaindigotone derivatives as cholinesterases inhibitors with multiple binding modes,[20] targeting both cholinesterases. However, their inhibition activities have been found to be lower than that of tacrine with only moderate inhibition selectivity for AChE over BuChE. In addition, the capability of isaindigotone derivatives to

* Corresponding authors. Tel./fax: +86 20 39943056.
E-mail addresses: tanjiah@mail.sysu.edu.cn (J.-H. Tan), ceshzs@mail.sysu.edu.cn (Z.-S. Huang).

0968-0896/$ - see front matter © 2012 Elsevier Ltd. All rights reserved.
doi:10.1016/j.bmc.2012.02.061

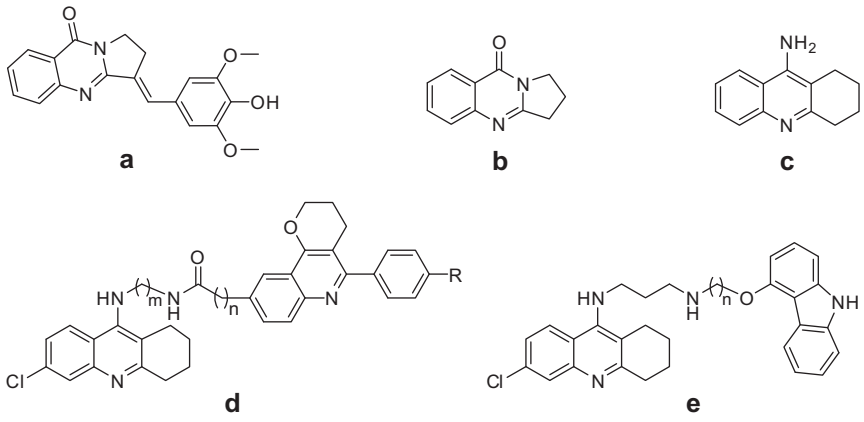

Figure 1. Chemical structures of isaindigotone (**a**), deoxyvasicinone (**b**), tacrine (**c**), and 6-chlorotacrine hybrids (**d**, **e**).

inhibit Aβ aggregation has not been investigated and the structural diversity of these compounds was not enough for the study of the structure–activity relationship of the interaction. Herein, we rationally designed and synthesized two new series of isaindigotone derivatives, and their inhibitory activities for cholinesterases (ChEs) and self-induced β-amyloid (Aβ) aggregation were investigated. It has been reported that the substitution of a chlorine atom at position 6 of tacrine and related compounds strongly increased the binding affinity of tacrine with AChE (**d** and **e**, Fig. 1).[21,22] Thus, we attached a chlorine atom at the similar position of our deoxyvasicinone moiety, in order to figure out whether the chlorine atom on the deoxyvasicinone moiety has the similar effect as the chlorine atom on tacrine in AChE inhibition. We also replaced the ether linkage of our previous compounds with N-phenylalkanamide or N-alkylbenzamide bond in order to increase their hydrogen bonding interaction. Our previous studies have shown that expanding the aliphatic ring size from five to six would resulted in decreased planarity of the aromatic core,[23] therefore, in the present study we varied the size of the aliphatic ring to investigate the effect of the planarity and linearity of the chromophore on their interactions with ChEs and Aβ. Molecular docking studies were carried out to study the binding mode and selectivity of these compounds for AChE, and the structure–activity relationships of these compounds were further investigated and discussed.

2. Results and discussion

2.1. Chemistry

Chloro-isaindigotone derivatives were facilely prepared according to the synthetic route as shown in Scheme 1. Most of the intermediates were prepared following the procedures reported in our previous work.[23,24] The synthesis began with commercially available 2-amino- 4-chlorobenzoic acid, which was dissolved in toluene and heated with pyrrolidin-2-one or piperidin-2-one in the presence of $POCl_3$. The intermediates (**2a, 2b**) were reacted with 4-nitrobenzaldehyde through Claisen–Schmidt condensation to provide the nitro intermediates (**3a, 3b**) at high yield.[25] The reduction of the nitro intermediates with sodium sulfide gave the amino intermediates (**4a, 4b**), which were subsequently treated with acyl chloride to give the chloro intermediates (**5a, 5b**). Their further amination with various alkylamines produced the desired compounds **6a–6h**. The carboxyl intermediates **(3c, 3d)** were obtained through the Claisen–Schmidt condensation of the intermediates (**2a, 2b**) with 4-formylbenzoic acid. The condensation of the carboxyl intermediates **(3c, 3d)** with various linear aliphatic amines catalyzed with BOP in DMF, gave the desired compounds **7a–7h**. NOESY experiments of compounds (**3a**–**3d**) showed the correlation between H-1 and H-2/H-2′, thus the double bond was assigned as the *E* configuration.

2.2. Inhibition studies of AChE and BuChE

The inhibitory activity of our synthetic compounds against AChE (from *electric eel*) and BuChE (from *equine serum*) was evaluated using the method of Ellman et al.,[26] with tacrine as a positive control. Their IC_{50} values and selectivity index for AChE over BuChE were summarized as shown in Table 1. Most of our compounds showed selective inhibition of AChE over BuChE, with IC_{50} values at micro or nano molar range. Obviously, the series **6** compounds with five-member aliphatic ring in the skeleton showed preferable inhibition and selectivity for AChE, suggesting that the more planar and linear chromophore was favored for occupying the PAS of AChE. The size of the aliphatic ring could impact the planarity and linearity of the skeleton, which may also adjust the orientation and rotation of the benzylidene moiety. We found that the compounds with various terminal amine groups in their side chains showed slightly different activity, and compound **6e** with piperidyl group exhibited optimal activity.

Comparing to the series **6** with the N-phenylalkanamides side chains, most of the series **7** compounds with the N-alkylbenzamides moiety exhibited decreased AChE inhibitory activity, except compound **7a**. These results indicated that electron-withdrawing effect of the N-alkylbenzamide bond may reduce the electronic density of the chromophore, and consequently, diminish the π–π stacking interaction between the chromophore and the PAS of AChE. On the other hand, some of series **7** compounds showed better BuChE inhibitory activity than series 6 compounds, such as compounds **7c** and **7g**. For BuChE, the peripheral site is surrounded with aliphatic amino acids instead of large aromatic residues for AChE, thus, the BuChE inhibition was weakly influenced by the reduction of electronic density of the chromophore.

2.3. Molecular modeling and kinetic studies

In order to study the binding mode and selectivity of our compounds with two cholinesterases, molecular modeling was carried out using the docking program AUTODOCK 4.0 package,[27] and the results were shown in Figure 2 with MOE 2008.10 software package.

Compound **6c**, with strong inhibitory activity and high selectivity to AChE, exhibited multiple binding modes with AChE, which were in agreement with those of our previous isaindigotone derivatives. The deoxyvasicinone moiety adopted an appropriate

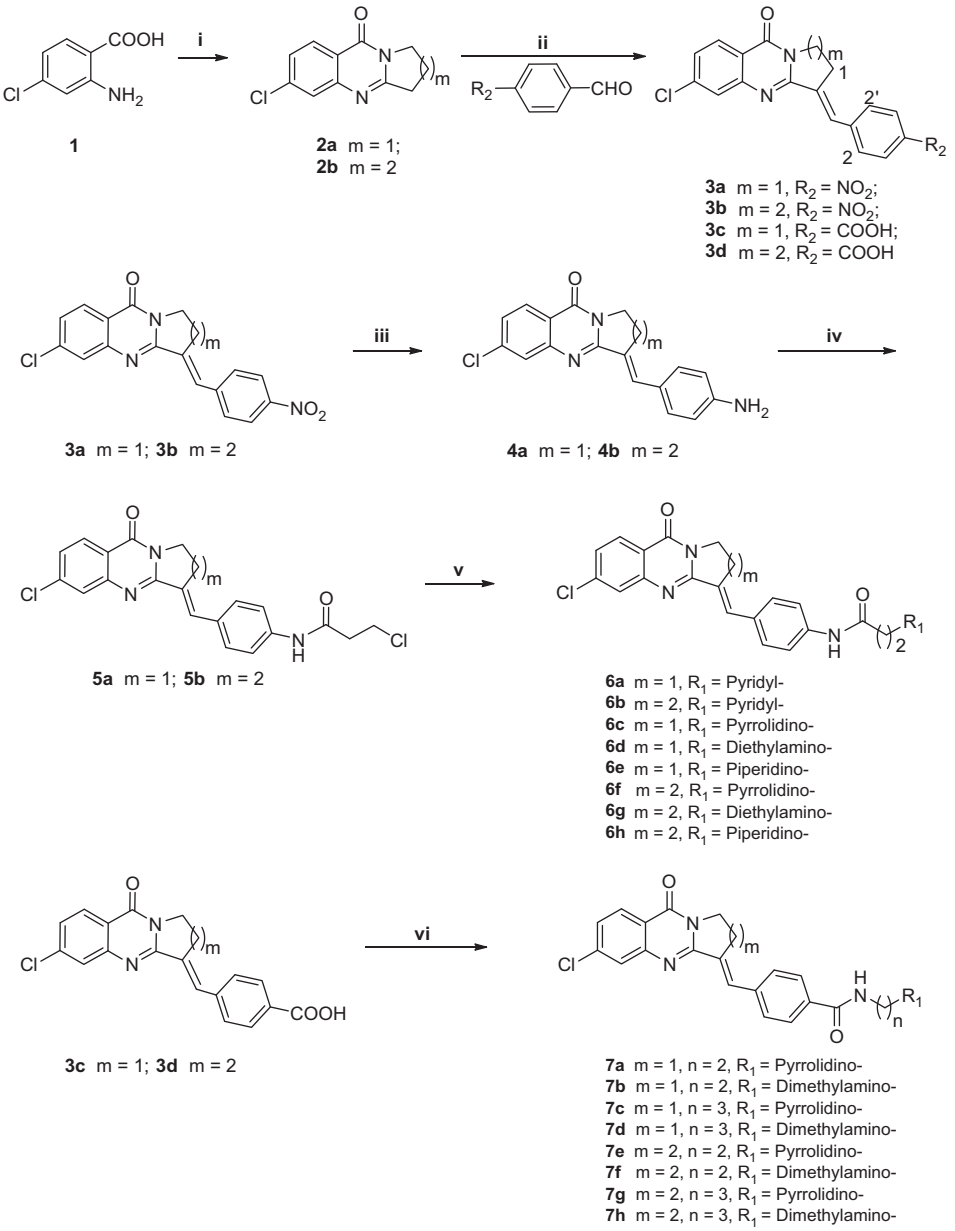

Scheme 1. Synthetic route for isaindigotone derivatives. Reagents and conditions: (i) toluene, $POCl_3$, 2-pyrrolidinone or piperidin-2-one, reflux; (ii) AcOH, AcONa, reflux; (iii) NaOH, $Na_2S{\cdot}9H_2O$, EtOH, reflux; (iv) CH_2Cl_2, 3-chloropropionyl chloride, reflux; (v) R_1H, KI, EtOH, reflux; (vi) $NH_2(CH_2)_nR_1$, BOP, triethylamine, DMF, 70 °C.

orientation for its binding to PAS, via the π–π stacking interaction with Trp279, and the ring-to-ring distance was 3.8 Å. But this preferred binding mode was different with that of 6-chlorotacrine, which interacted with CAS, and no significant interaction between chlorine atom of the deoxyvasicinone moiety with the residues of PAS was found. The binding affinity can be attributed to the π–π stacking interaction between the benzylidene moiety and Phe331 with a distance of 3.8 Å. The conformation of the side chain could fit well with the shape of the gorge. The positively-charged nitrogen of pyrrolidine made a cation–π interaction (4.5 Å) with Trp84, and the hydrogen on the nitrogen of pyrrolidine was hydrogen-bonded with Glu199 with a distance of 2.9 Å. These results may rationalize the potent inhibition of compound **6c** for AChE. On the other hand, compound **6c** could also occupy the large catalytic cavity of *Hu*BuChE, but without strong interactions except a hydrogen bond between Glu197 and the hydrogen on the nitrogen of pyrrolidine. Meanwhile, the calculated binding free energy of compound **6c** with AChE is much lower than that with *Hu*BuChE (−12.74 and −10.48 Kcal/mol, respectively), thus, compound **6c** exhibited excellent selectivity for the inhibition of AChE over BuChE.

We also performed the docking studies of compound **7c** with AChE (shown in Supplementary data). From the docking result, only the cation–π interaction between positively-charged nitrogen of pyrrolidine and Trp84 was observed, and no stacking interaction between the chromophore and the PAS of AChE was found. This result supported that the electron-withdrawing effect of the N-alkylbenzamide bond may reduce the π–π stacking interaction between the chromophore and the PAS of AChE.

The nature of AChE inhibition of compound **6c** was further investigated using graphical analysis of steady-state inhibition data.[28] As shown in Figure 3, a mixed type of inhibition was confirmed, which indicated that compound **6c** could bind to both

Table 1
Inhibition IC_{50} values and selectivity index of isaindigotone derivatives on AChE and BuChE

Compound	R_1	n	m	IC_{50} (nM)		Selectivity[c] for AChE
				AChE[a]	BuChE[b]	
6a		–	1	49 ± 7	1700 ± 490	35
6b		–	2	820 ± 350	3380 ± 270	4.12
6c		–	1	41 ± 14	3820 ± 260	93
6f		–	2	>1000	6450 ± 680	–
6d		–	1	60 ± 1	6440 ± 900	107
6g		–	2	>1000	2340 ± 410	–
6e		–	1	23 ± 3	2880 ± 340	130
6h		–	2	31 ± 1	5990 ± 110	190
7a		2	1	45 ± 7	11060 ± 830	250
7c		3	1	1440 ± 730	610 ± 120	0.42
7e		2	2	1510 ± 290	6750 ± 2300	4.5
7g		3	2	1210 ± 140	500 ± 80	0.4
7b		2	1	160 ± 0	>20000	>125
7d		3	1	1420 ± 540	5180 ± 260	3.6
7f		2	2	360 ± 70	>40000	>111
7h		3	2	2050 ± 280	6640 ± 730	3.2
Tacrine				96 ± 2	14 ± 1	0.15

[a] Inhibitor concentration (mean _ SEM of three experiments) required for 50% inactivation of AChE.
[b] Inhibitor concentration (mean _ SEM of three experiments) required for 50% inactivation of BuChE.
[c] Selectivity for AChE: IC_{50} (BuChE)/IC_{50} (AChE).

PAS and CAS of AChE. This result was in agreement with the results of molecular modeling studies.

2.4. Inhibition of self-mediated $A\beta_{1-40}$ aggregation

To investigate the activity of our compounds to inhibit the self-mediated $A\beta_{1-40}$ aggregation, the Thioflavin T (ThT) fluorescence assay was performed.[29] As shown in Table 2, most of our compounds showed better inhibitory activity of $A\beta_{1-40}$ aggregation at 10 μM compared to the reference compound curcumin. Interestingly, compound **6c** with excellent inhibitory activity and high selectivity to AChE, also gave the optimal inhibition of $A\beta_{1-40}$ aggregation (62.31%) at 10 μM, which indicated that our compounds were dual inhibitors for AChE and Aβ aggregation.

2.5. Effect of compound 6c on Aβ β-sheet formation

It has been reported that Aβ comprises a conformational mixture of α-helix, β-sheet, and random coil in the aqueous solution, and forms intramolecular β-sheet structure in the fibrillation through a conformational change.[30] CD spectroscopy was employed to study the effect of compound **6c** on the structural change of $A\beta_{1-40}$. As shown in Figure 4, there was no aggregation for $A\beta_{1-40}$ (black and red line) before incubation. After 3 days incubation, the CD spectrum of $A\beta_{1-40}$ alone (blue line) was found to have a negative band around 217 nm and positive band around 197 nm, which were assigned to α-helix structure and β-sheet structure, respectively. Notably, the addition of compound **6c** (green line) led to significant decrease of the band around 197 nm, with slight change to the intensity of the band around 217 nm. These results revealed that compound **6c** could reduce the β-sheet structure formation, without significant effect on the content of α-helix structure.

2.6. Effect of compound 6c on abundance of Aβ fibrils

Finally, electron microscopy (EM) was employed to monitor and clarify the effect of compound **6c** on Aβ aggregation. As shown in Figure 5, the control sample of $A\beta_{1-40}$ alone was mostly aggregated into mature and bulky amyloid fibrils after 4 days of incubation. In contrast, only a few short fibrils were found for the $A\beta_{1-40}$ sample incubated with compound **6c**. This EM experimental result showed that compound **6c** could inhibit the $A\beta_{1-40}$ fibrils formation, which was in agreement with the results from ThT and CD studies.

3. Conclusion

In summary, two new series of chloro-substituted isaindigotone derivatives and analogues were synthesized as dual inhibitors for AChE and amyloid beta aggregation. Some of these compounds were found to have improved inhibitory activity and selectivity for AChE compared with the isaindigotone derivatives developed previously in our group. The structure–activity relationship studies revealed that the compounds containing the five-member aliphatic ring had higher inhibition activity on AChE and much higher selectivity for AChE over BuChE, compared to the compounds with the six-member aliphatic ring. Most compounds showed higher self-induced Aβ aggregation inhibitory activity than a reference compound curcumin. Further investigation of compound **6c** through CD and EM experiments confirmed that compound **6c** could reduce or inhibit β-sheet aggregation and fibril formation. Our present results indicated that isaindigotone derivatives could become lead compounds for further development for new anti-Alzheimer agents.

4. Experimental section

4.1. Chemistry

^1H and ^{13}C NMR spectra were recorded using TMS as the internal standard in $CDCl_3$ or DMSO-d_6 with a Bruker BioSpin GmbH spectrometer at 400 MHz and 100 MHz, respectively. High resolution mass spectra (HRMS) were recorded on Shimadzu LCMS-IT-TOF. Flash column chromatography was performed with silica gel (200–300 mesh) purchased from Qingdao Haiyang Chemical Co. Ltd. The purity of synthesized compounds was confirmed to be higher than 95% through analytical HPLC performed with a dual pump Shimadzu LC-20AB system equipped with an Ultimate XB-C18 column (4.6 × 250 mm, 5 μm) and eluted with methanol/water (40:60 to 60:40) containing 0.1% TFA at a flow rate of 0.5 mL/min. All chemicals were purchased from commercial

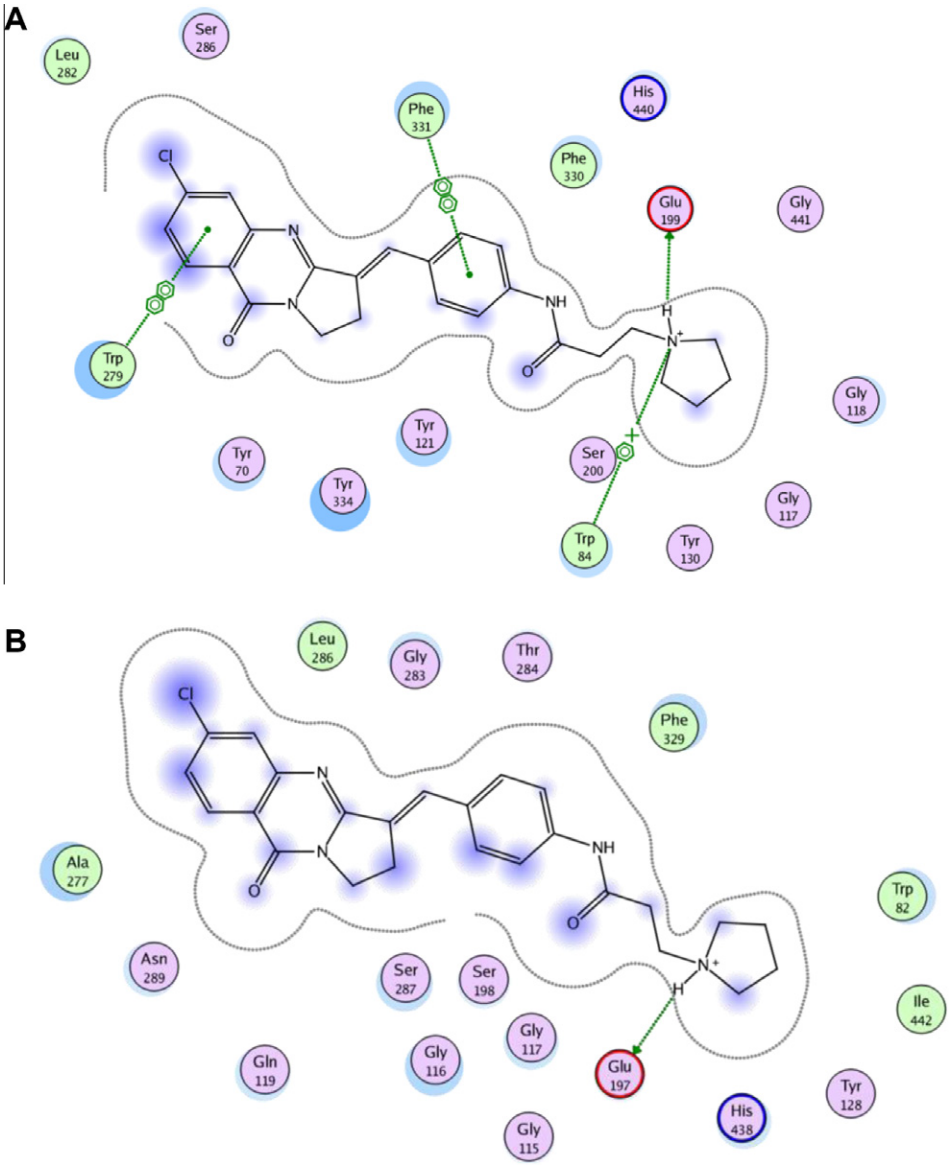

Figure 2. Docking models of compound **6c** with *Tc*AChE (A) and *Hu*BuChE (B) generated with MOE.

sources unless otherwise specified. All the solvents were of analytical reagent grade and were used without further purification.

4.2. Synthesis of intermediate 2a–2b

4.2.1. 6-Chloro-2,3-dihydropyrrolo[2,1-*b*]quinazolin-9(1*H*)-one (2a)

To a solution of 2-pyrrolidinone (6.01 g, 60 mmol) and 2-amino-4-chlorobenzoic acid **1** (3.36 g, 20 mmol) in 50 mL anhydrous toluene, phosphorus oxychloride (11 mL) was added dropwise at room temperature. The mixture was then stirred under reflux for 5 h. After concentrating to give a slurry, the residue was poured onto ice, and then aqueous NaOH was added to make the solution basic. The mixture was extracted with three 100 mL portions of EtOAc. The combine organic phase was washed with 80 mL water, dried over magnesium sulfate, and concentrated under reduced pressure. The crude product was purified by using flash column chromatography with EtOAc/petroleum ether (1:4) elution to afford a white solid compound **2a** (2.91 g, 63.0%): ^{1}H NMR (400 MHz, $CDCl_3$): δ 8.19 (d, J = 8.5 Hz, 1H), 7.62 (d, J = 2.0 Hz, 1H), 7.39 (dd, J = 8.5, 2.0 Hz, 1H), 4.20 (t, J = 8.0 Hz, 2H), 3.18 (t, J = 8.0 Hz, 2H), 2.35–2.25 (m,2H). LC-MS m/z: 221 $[M+H]^+$.

4.2.2. 3-Chloro-8,9-dihydro-6*H*-pyrido[2,1-*b*]quinazolin-11(7*H*)-one (2b)

Following the method for preparation of **2a**, 2-pyrrolidinone was replaced with piperidin-2-one, and a white solid **2b** was obtained (2.98 g, 64.4%): ^{1}H NMR (400 MHz, $CDCl_3$): δ 8.18 (d, J = 8.6 Hz, 1H), 7.59 (d, J = 1.9 Hz, 1H), 7.37 (dd, J = 8.6, 2.0 Hz, 1H), 4.06 (t, J = 6.2 Hz, 2H), 2.99 (t, J = 6.7 Hz, 2H), 2.06–1.91 (m, 4H). LC-MS m/z: 235 $[M+H]^+$.

4.3. General procedures for the preparation of compounds (3a–3d)

A mixture of **2a/2b** (10 mmol), different aromatic aldehyde (11 mmol) and AcOH (30 mL), sodium acetate (8 mmol) was heated under reflux for 10–24 h. After cooling to room temperature, the mixture was filtered and washed with water, CH_2Cl_2, and EtOH, to give desired compounds.

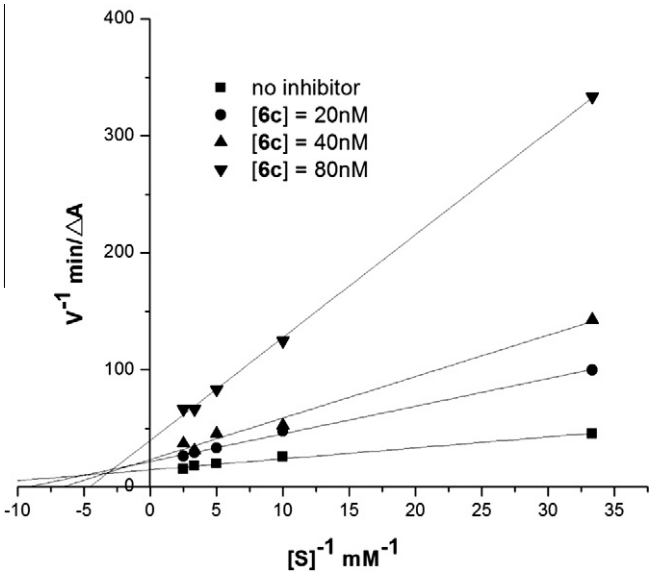

Figure 3. Lineweaver-Burk plot for the inhibition of AChE by compound **6c**.

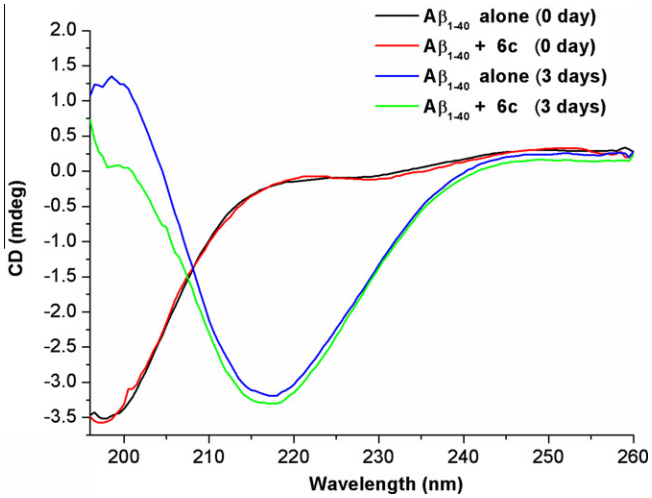

Figure 4. CD spectroscopy of $A\beta_{1-40}$ alone and with compound **6c** incubated for 0 or 3 days.

4.3.1. (*E*)-6-chloro-3-(4-nitrobenzylidene)-2,3-dihydropyrrolo [2,1-*b*]quinazolin-9(1*H*)-one (3a)

Intermediate **2a** was treated with 4-nitrobenzaldehyde according to general procedure to give the desired product **3a** as pale yellow solid (2.37 g, 67.1%). ^{1}H NMR (400 MHz, DMSO-d_6): δ 8.30 (d, J = 8.6 Hz, 2H), 8.15 (d, J = 8.5 Hz, 1H), 7.94 (d, J = 8.6 Hz, 2H), 7.83 (s, 1H), 7.78 (d, J = 1.6 Hz, 1H), 7.55 (dd, J = 8.2, 1.7 Hz, 1H), 4.21 (t, J = 7.0 Hz, 2H), 3.38–3.32 (m, 2H).. LC-MS *m/z*: 354 $[M+H]^+$.

4.3.2. (*E*)-3-Chloro-6-(4-nitrobenzylidene)-8,9-dihydro-6*H*-pyrido[2,1-*b*]quinazolin-11(7*H*)-one (3b)

Intermediate **2b** was treated with 4-nitrobenzaldehyde according to general procedure to give the desired product **3b** as pale yellow solid (2.35 g, 63.9%). ^{1}H NMR (400 MHz, $CDCl_3$): δ 8.32–8.27 (m, 3H), 8.22 (d, J = 8.5 Hz, 1H), 7.74 (d, J = 1.8 Hz, 1H), 7.62 (d, J = 8.5 Hz, 2H), 7.42 (dd, J = 8.6, 2.0 Hz, 1H), 4.18 (t, J = 8.0 Hz, 2H), 2.99–2.90 (m, 2H), 2.12–2.03 (m, 2H). LC-MS *m/z*: 368 $[M+H]^+$.

4.3.3. (*E*)-4-((6-Chloro-9-oxo-1,2-dihydropyrrolo[2,1-*b*] quinazolin-3(9*H*)-ylidene)methyl) benzoic acid (3c)

Intermediate **2a** was treated with 4-formylbenzoic acid according to general procedure to give the desired product **3c** as pale yellow solid (2.31 g, 65.6%). ^{1}H NMR (400 MHz, DMSO-d_6): δ 13.14 (s, 1H), 8.13 (d, J = 8.5 Hz, 1H), 8.02 (d, J = 8.3 Hz, 2H), 7.83–7.73 (m, 4H), 7.53 (dd, J = 8.5, 1.8 Hz, 1H), 4.19 (t, J = 7.0 Hz, 2H), 3.38–3.29 (m, 3H). LC-MS *m/z*: 353 $[M+H]^+$.

4.3.4. (*E*)-4-((3-Chloro-11-oxo-7,8,9,11-tetrahydro-6*H*-pyrido [2,1-*b*]quinazolin-6-ylidene) methyl) benzoic acid (3d)

Intermediate **2b** was treated with 4-formylbenzoic acid according to general procedure to give the desired product **3d** as yellow solid (2.45 g, 66.8%). ^{1}H NMR (400 MHz, DMSO-d_6): δ 13.02 (s, 1H), 8.20 (s, 1H), 8.11 (d, J = 8.6 Hz, 1H), 8.01 (d, J = 8.1 Hz, 2H), 7.74 (s, 1H), 7.65 (d, J = 8.0 Hz, 2H), 7.51 (d, J = 8.5 Hz, 1H), 4.04 (t, J = 6.0 Hz, 2H), 2.91 (t, J = 5.4 Hz, 2H), 2.01–1.93 (m, 2H). LC-MS *m/z*: 367 $[M+H]^+$.

4.4. Synthesis of intermediate 4a–4b

4.4.1. (*E*)-3-(4-Aminobenzylidene)-6-chloro-2,3-dihydropyrrolo [2,1-*b*]quinazolin-9(1*H*)-one (4a)

To a stirred suspension of **3a** (3.5 g,10 mmol) in ethanol (50 mL) was added a solution of $Na_2S.9H_2O$ (12 g, 50 mmol) and NaOH (8 g, 200 mmol) in water (100 mL). The mixture was heated at 90 °C for 8 h. The ethanol was removed under vacuo. After cooling to room temperature, the precipitate was collected through filtration, repeatedly washed with water and ethanol, and dried, to afford the product **4a** (2.05 g, 64.3%). ^{1}H NMR (400 MHz, DMSO-d_6): δ 8.07 (d, J = 8.5 Hz, 1H), 7.66 (d, J = 2.0 Hz, 1H), 7.57 (t, J = 2.3 Hz, 1H), 7.42 (dd, J = 8.5, 2.0 Hz, 1H), 7.35 (d, J = 8.6 Hz, 2H), 6.65 (d, J = 8.5 Hz, 2H), 5.79 (s, 2H), 4.14 (t, J = 6.0 Hz, 2H), 3.21–3.11 (m, 2H). LC-MS *m/z*: 324 $[M+H]^+$.

4.4.2. (*E*)-6-(4-Aminobenzylidene)-3-chloro-8,9-dihydro-6*H*-pyrido[2,1-*b*]quinazolin-11(7*H*)-one (4b)

Following the method for preparation of **4a**, a red solid **4b** (2.23 g, 66.1%) was obtained. ^{1}H NMR (400 MHz, $CDCl_3$): δ 8.22–8.10 (m, 2H), 7.69 (d, J = 1.7 Hz, 1H), 7.41–7.30 (m, 3H), 6.71 (d, J = 8.4 Hz, 2H), 4.14 (t, J = 8.0 Hz, 2H), 3.91 (s, 2H), 2.95 (t, J = 6.3 Hz, 2H), 2.11–1.95 (m, 2H). LC-MS *m/z*: 338 $[M+H]^+$.

4.5. Synthesis of intermediate (5a–5b)

4.5.1. (*E*)-3-Chloro-*N*-(4-((6-chloro-9-oxo-1,2-dihydropyrrolo[2,1-*b*]quinazolin-3(9*H*)-ylidene) methyl)phenyl)propanamide (5a)

To a stirred suspension of **4a** (0.96 g, 3 mmol) in CH_2Cl_2 (20 mL), 3-chloropropanoyl chloride (1 mL, 12 mmol) was added. The

Table 2
Inhibition of self-induced $A\beta_{1-40}$ aggregation by isaindigotone derivatives with curcumin as a reference

Compound	Inhibition ratio (%)	Compound	Inhibition ratio (%)	Compound	Inhibition ratio (%)	Compound	Inhibition ratio (%)
6a	49/96 ± 4.45	6e	49.80 ± 4.86	**7a**	57.39 ± 2.13	**7e**	53.60 ± 3.57
6b	32.96 ± 2.55	6f	53.46 ± 2.03	**7b**	36.84 ± 6.76	**7f**	54.47 ± 3.44
6c	62.31 ± 0.28	6g	54.76 ± 3.97	**7c**	36.25 ± 2.65	**7g**	53.28 ± 1.78
6d	39.00 ± 1.42	6h	52.94 ± 3.70	**7d**	56.46 ± 1.60	**7h**	49.75 ± 3.60
Curcumin	48.76 ± 0.83						

The ThT method was used, the mean ± SD of three independent experiments and the measurements were carried out in presence of 10 μM compounds.

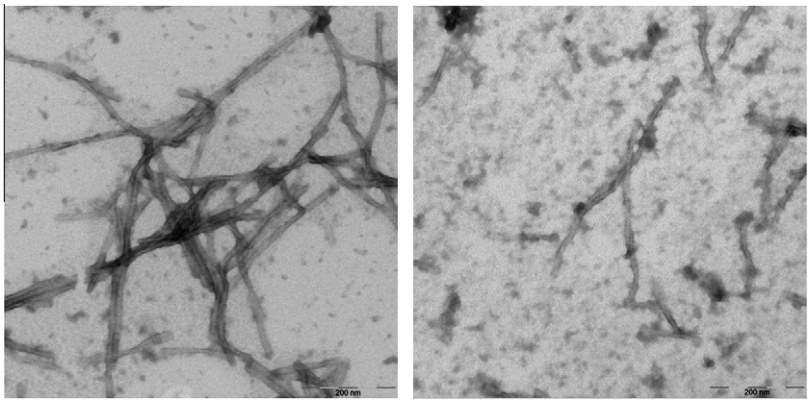

Figure 5. EM images of $A\beta_{1-40}$ (100 μM) in the absence (left) and presence (right) of 10 μM compound **6c**, after 4 days of incubation.

mixture was then heated under reflux for 6 h. After cooling to room temperature, the precipitate was separated from solvent through filtration and washed with ethanol to afford a yellow solid **5a** (1.13 g, 90.9%). ^{1}H NMR (400 MHz, DMSO-d_6): δ 10.40 (s, 1H), 8.12 (d, J = 8.5 Hz, 1H), 7.79–7.69 (m, 4H), 7.64 (d, J = 8.4 Hz, 2H), 7.50 (d, J = 7.0 Hz, 1H), 4.18 (t, J = 8.0 Hz, 2H), 3.90 (t, J = 6.0 Hz, 2H), 3.27 (t, J = 6.0 Hz, 2H), 2.88 (t, J = 6.0 Hz, 2H). LC-MS m/z: 414 $[M+H]^+$.

4.5.2. (*E*)-4-Chloro-N-(4-((3-chloro-11-oxo-7,8,9,11-tetrahydro-6*H*-pyrido[2,1-*b*]quinazolin-6-ylidene)methyl)phenyl)butanamide (5b)

Following the method for preparation of **5a**, a yellow solid **5b** (1.07 g, 83.3%) was obtained. ^{1}H NMR (400 MHz, DMSO-d_6): δ 10.34 (s, 1H), 8.16–8.07 (m, 2H), 7.79–7.69 (m, 3H), 7.55 (d, J = 8.4 Hz, 2H), 7.49 (dd, J = 8.6, 1.3 Hz, 1H), 4.05 (t, J = 6.0 Hz, 2H), 3.90 (t, J = 6.2 Hz, 2H), 2.92 (t, J = 5.8 Hz, 2H), 2.87 (t, J = 6.2 Hz, 2H), 2.03–1.90 (m, 2H). LC-MS m/z: 428 $[M+H]^+$.

4.6. General procedure for the preparation of compounds (6a–6h)

To a stirred suspension of **5a**/**5b** (0.25 g, 0.5 mmol) and KI (0.05 g) in EtOH (7 mL), different amine (2.5 mmol) was added dropwise. The mixture was stirred under reflux for 3–6 h. After cooling to 0 °C, the precipitate was collected through filtration and washed with water and ethanol, to give desired products **6a–6h**.

4.6.1. (*E*)-*N*-(4-((6-Chloro-9-oxo-1,2-dihydropyrrolo[2,1-*b*]quinazolin-3(9*H*)-ylidene)methyl) phenyl)-3-(pyrrolidin-1-yl)propanamide (6c)

Intermediate **5a** was reacted with pyrrolidine following the general procedure to give the desired product **6c** as an orange solid with a yield of 66.8%. Mp 237–240 °C. ^{1}H NMR (400 MHz, $CDCl_3$): δ 11.62 (s, 1H), 8.21 (d, J = 8.5 Hz, 1H), 7.79 (s, 1H), 7.73 (d, J = 1.6 Hz, 1H), 7.59 (d, J = 8.5 Hz, 2H), 7.53 (d, J = 8.5 Hz, 2H), 7.37 (dd, J = 8.5, 1.7 Hz, 1H), 4.29 (t, J = 7.3 Hz, 2H), 3.29 (t, J = 6.0 Hz, 2H), 2.88 (t, J = 8.0 Hz, 2H), 2.77–2.65 (m, 4H), 2.57 (t, J = 6.0 Hz, 2H), 1.99–1.86 (m, 4H). ^{13}C NMR (100 MHz, $CDCl_3$): δ 171.03, 160.67, 150.99, 150.89, 140.32, 139.89, 131.17, 130.88, 130.53, 129.42, 127.75, 126.70, 126.44, 119.66, 119.29, 53.10, 51.26, 44.10, 34.65, 25.47, 23.75. Purity: 98.8% by HPLC. LC-MS m/z: 449 $[M+H]^+$. HRMS (ESI): calcd for $(M+H)^+$ ($C_{25}H_{25}N_4O_2Cl$) 449.1739, found 449.1731.

4.7. General procedure for preparation of compounds (7a–7h)

A mixture of **3c**/**3d** (1 mmol), BOP (0.66 g, 1.5 mmol), triethylamine (0.28 ml, 2 mmol), different amine (2 mmol) and DMF(10 ml) was heated at 70 °C for 12–20 h. After cooling to room temperature, the mixture was filtered. The filtrate was washed with water and methanol, to give desired products **7a–7h**.

4.8. Biological assay

4.8.1. In vitro AChE and BuChE inhibition assay

Acetylcholinesterase (AChE, E.C. 3.1.1.7, from *electric eel*), butyrylcholinesterase (BuChE, E.C. 3.1.1.8, from *equine serum*), 5,5′-dithiobis-(2-nitrobenzoic acid) (Ellman's reagent, DTNB), acetylthiocholine chloride (ATC), butyrylthiocholine chloride (BTC) were purchased from Sigma–Aldrich. Isaindigotone derivatives were dissolved in DMSO and then diluted in 0.1 M KH_2PO_4/K_2HPO_4 buffer (pH 8.0) to provide a final concentration range.

All the assays were carried out in 0.1 M KH_2PO_4/K_2HPO_4 buffer, pH 8.0, using a Shimadzu 2450 Spectrophotometer. Enzyme solutions were prepared at the concentration of 2.0 unit/mL. The assay medium contained phosphate buffer (pH 8.0), 0.01 M DTNB, AChE, and 0.01 M substrate (ATC). The substrate was added to the medium with inhibitor after incubation for 15 min. The activity was determined by measuring the increase in absorbance at 412 nm in 1 min interval at 37 °C. The data were calculated based on the method of Ellman et al. In vitro BuChE assays were carried out using a similar method as described above.[26]

4.8.2. Molecular modeling studies

The crystal structure of the torpedo acetylcholinesterase complexed with tacrine (code ID: 1ACJ) and the human butyrylcholinesterase complexed with echothiophate (code ID: 1POI) were obtained from the Protein Data Bank after removing the inhibitor and water molecules. The 3D structure of compound **6c** was built, and its geometry optimization was performed with molecular mechanics. Further preparation of substrates included addition of Gasteiger charges, removal of hydrogen atoms and addition of their atomic charges to skeleton atoms, and finally, assignment of proper atomic types. Autotors was then used to define the rotatable bonds in the ligand.

Docking studies were carried out using the AUTODOCK 4.0 program. By using ADT, polar hydrogen atoms were added to amino acid residues and Gasteiger charges were assigned to all atoms of the enzyme. The resulting enzyme structure was used as an input for the AUTOGRID program. AUTOGRID performed a pre-calculated atomic affinity grid maps for each atom type in the ligand plus an electrostatics map and a separate desolvation map present in the substrate molecule. All maps were calculated with 0.375 Å spacing between grid points. Flexible ligand docking was performed for the compound. Docking calculations were carried out using the

Lamarckian genetic algorithm (LGA), and all parameters were the same for each docking. The results were shown with Molecular Operating Environment (MOE) program (Chemical Computing Group, Montreal, Canada).

4.8.3. Kinetic studies of AChE inhibition

Kinetic characterization of AChE was performed using a reported method.[28] Compound **6c** was added into the assay solution and pre-incubated with the enzyme at 37 °C for 15 min, followed by the addition of ATC. The assay solution (200 μL) containing compound **6c** (20, 40, 80 nM), DTNB (0.5 mM), 10 μL AChE and ATC (0.03, 0.1, 0.2, 0.3, 0.4 mM) dissolved in 0.1 M KH_2PO_4/K_2HPO_4 buffer (pH 8.0). Kinetic characterization for the hydrolysis of ATC catalyzed by AChE was carried out spectrometrically at 412 nm. The parallel control experiment was carried out without compound **6c** in the mixture.

4.8.4. Inhibition of $A\beta_{1-40}$ self-induced aggregation

The Thioflavin T fluorescence method was used,[29] and $A\beta_{1-40}$ peptide (Anaspec Inc) was dissolved in phosphate buffer (pH 7.4, 0.1 M) to give a 100 μM solution. Compounds were firstly dissolved in DMSO at a concentration of 10 mM. The final concentration of $A\beta_{1-40}$ and compounds were 50 μM and 10 μM, respectively. After incubating at 37 °C for 72 h, Thioflavin T (5 μM in 50 mM glycine-NaOH buffer, pH 8.0) was added. Fluorescence was measured at 450 nm (λ_{ex}) and 485 nm (λ_{em}). Each compound was examined in triplicate. The fluorescence intensities were recorded, and the percentage of inhibition on aggregation was calculated with the following equation: $(1-I_{Fi}/I_{Fc}) \times 100\%$ in which I_{Fi} and I_{Fc} were the fluorescence intensities obtained for absorbance in the presence and absence of inhibitors, respectively, after subtracting the background fluorescence of the 5 μM Thioflavin T solution.

4.8.5. CD assay

$A\beta_{1-40}$ (100 μM) was mixed with and without 20 μM compound **6c** in 0.1 M phosphate buffer (pH 7.4). All solutions were incubated at 37 °C for 3 days. CD spectra were obtained using a Jasco-810-150S spectropolarimeter (Jasco, Japan). A quartz cell with 1 mm optical path was used. Spectra were recorded at 25 °C between 195 and 255 nm with a bandwidth of 0.5 nm, a 3 s response time and scan speed of 10 nm/min.

4.8.6. EM assay

$A\beta_{1-40}$ peptide (Anaspec Inc) was dissolved in 0.1 M phosphate buffer (pH 7.4), which was incubated in the presence and absence of **6c** at 37 °C. The final concentrations of $A\beta_{1-40}$ and **6c** were 100 μM and 10 μM, respectively. After 4 days incubation, aliquots of 10 μL samples were placed on carbon-coated copper/rhodium grid. After 1 min, the grid was washed with water and negatively stained with 2% uranyl acetate solution for 1 min. After draining off the excess of staining solution by means of a filter paper, the specimen was transferred for examination in a transmission electron microscope (JEOL JEM-1400).

Acknowledgements

This work was supported by National Natural Science Foundation of China (No. 90813011, 21172272, 81001400), the International S&T Cooperation Program of China (No. 2010DFA34630).

Supplementary data

Supplementary data (the preparation of the compounds, ^1H NMR, ^{13}C NMR, HPLC and HRMS spectra of target compounds (**6a**–**6h**, **7a**–**7h**), NOSEY spectra of compounds (**3a**–**3d**), and docking result of compound **7c** with AChE) associated with this article can be found, in the online version, at doi:10.1016/j.bmc.2012.02.061.

References and notes

1. Forstl, H.; Kurz, A. *Eur. Arch. Psy. Clin. N.* **1999**, *249*, 288.
2. Cummings, J. L. *N. Engl. J. Med.* **1912**, *2004*, 351.
3. Alzheimer's Association. http://www.alz.org/national/documents/report_alzfactsfi-gures2009.pdf. **2009**.
4. Citron, M. *Nat. Rev. Neurosci.* **2004**, *5*, 677.
5. Citron, M. *Nat. Rev. Drug Discov.* **2010**, *9*, 387.
6. Ferris, S. H. *Expert Opin. Pharmacother.* **2003**, *4*, 2305.
7. Cavalli, A.; Bolognesi, M. L.; Minarini, A.; Rosini, M.; Tumiatti, V.; Recanatini, M.; Melchiorre, C. *J. Med. Chem.* **2008**, *51*, 347.
8. Ibach, B.; Haen, E. *Curr. Pharm. Des.* **2004**, *10*, 231.
9. Inestrosa, N. C.; Alvarez, A.; Perez, C. A.; Moreno, R. D.; Vicente, M.; Linker, C.; Casanueva, O. I.; Soto, C.; Garrido, J. *Neuron* **1996**, *16*, 881.
10. Kryger, G.; Silman, I.; Sussman, J. L. *Struct. Fold. Des.* **1999**, *7*, 297.
11. Ono, K.; Condron, M. M.; Ho, L.; Wang, J.; Zhao, W.; Pasinetti, G. M.; Teplow, D. B. *J. Biol. Chem.* **2008**, *283*, 32176.
12. Narlawar, R.; Baumann, K.; Schubenel, R.; Schmidt, B. *Neurodegener. Dis.* **2007**, *4*, 88.
13. Zhou, Y.; Jiang, C.; Zhang, Y.; Liang, Z.; Liu, W.; Wang, L.; Luo, C.; Zhong, T.; Sun, Y.; Zhao, L.; Xie, X.; Jiang, H.; Zhou, N.; Liu, D.; Liu, H. *J. Med. Chem.* **2010**, *53*, 5449.
14. Rizzo, S.; Riviere, C.; Piazzi, L.; Bisi, A.; Gobbi, S.; Bartolini, M.; Andrisano, V.; Morroni, F.; Tarozzi, A.; Monti, J. P.; Rampa, A. *J. Med. Chem.* **2008**, *51*, 2883.
15. Fernandez-Bachiller, M. I.; Perez, C.; Campillo, N. E.; Paez, J. A.; Gonzalez-Munoz, G. C.; Usan, P.; Garcia-Palomero, E.; Lopez, M. G.; Villarroya, M.; Garcia, A. G.; Martinez, A.; Rodriguez-Franco, M. I. *ChemMedChem* **2009**, *4*, 828.
16. Li, Y. P.; Ning, F. X.; Yang, M. B.; Li, Y. C.; Nie, M. H.; Ou, T. M.; Tan, J. H.; Huang, S. L.; Li, D.; Gu, L. Q.; Huang, Z. S. *Eur. J. Med. Chem.* **2011**, *46*, 1572.
17. Wu, X. Y.; Qin, G. W.; Cheung, K. K.; Cheng, K. F. *Tetrahedron* **1997**, *53*, 13323.
18. Decker, M.; Krauth, F.; Lehmann, J. *Bioorg. Med. Chem.* **1966**, *2006*, 14.
19. Decker, M. *J. Med. Chem.* **2006**, *49*, 5411.
20. Pan, L.; Tan, J. H.; Hou, J. Q.; Huang, S. L.; Gu, L. Q.; Huang, Z. S. *Bioorg. Med. Chem. Lett.* **2008**, *18*, 3790.
21. Rosini, M.; Simoni, E.; Bartolini, M.; Cavalli, A.; Ceccarini, L.; Pascu, N.; McClymont, D. W.; Tarozzi, A.; Bolognesi, M. L.; Minarini, A.; Tumiatti, V.; Andrisano, V.; Mellor, I. R.; Melchiorre, C. *J. Med. Chem.* **2008**, *51*, 4381.
22. Camps, P.; Formosa, X.; Galdeano, C.; Munoz-Torrero, D.; Ramirez, L.; Gomez, E.; Isambert, N.; Lavilla, R.; Badia, A.; Clos, M. V.; Bartolini, M.; Mancini, F.; Andrisano, V.; Arce, M. P.; Rodriguez-Franco, M. I.; Huertas, O.; Dafni, T.; Luque, F. J. *J. Med. Chem.* **2009**, *52*, 5365.
23. Hou, J. Q.; Tan, J. H.; Wang, X. X.; Chen, S. B.; Huang, S. Y.; Yan, J. W.; Chen, S. H.; Ou, T. M.; Luo, H. B.; Li, D.; Gu, L. Q.; Huang, Z. S. *Org. Biomol. Chem.* **2011**, *9*, 6422.
24. Tan, J. H.; Ou, T. M.; Hou, J. Q.; Lu, Y. J.; Huang, S. L.; Luo, H. B.; Wu, J. T.; Huang, Z. S.; Wong, K. Y.; Gu, L. Q. *J. Med. Chem.* **2009**, *52*, 2825.
25. Molina, P.; Tarraga, A.; Gonzalez-Tejero, A.; Rioja, I.; Ubeda, A.; Terencio, M. C.; Alcaraz, M. J. *J. Nat. Prod.* **2001**, *64*, 1297.
26. Ellman, G. L.; Courtney, K. D.; Andres, V., Jr.; Feather-Stone, R. M. *Biochem. Pharmacol.* **1961**, *7*, 88.
27. Morris, G. M.; Goodsell, D. S.; Halliday, R. S.; Huey, R.; Hart, W. E.; Belew, R. K.; Olson, A. J. *J. Comput. Chem.* **1998**, *19*, 1639.
28. Tang, H.; Ning, F. X.; Wei, Y. B.; Huang, S. L.; Huang, Z. S.; Chan, A. S.; Gu, L. Q. *Bioorg. Med. Chem. Lett.* **2007**, *17*, 3765.
29. LeVine, H. *Protein sci.* **1993**, *2*, 404.
30. Pratim Bose, P.; Chatterjee, U.; Nerelius, C.; Govender, T.; Norstrom, T.; Gogoll, A.; Sandegren, A.; Gothelid, E.; Johansson, J.; Arvidsson, P. I. *J. Med. Chem.* **2009**, *52*, 8002.